Otology & Neurotology
34:1675–1680 © 2013, Otology & Neurotology, Inc.

Analysis of Intersubject Variations in Intracochlear and Middle Ear Surface Anatomy for Cochlear Implantation

*Stanley Pelosi, †Jack H. Noble, †Benoit M. Dawant, and *Robert F. Labadie

**Department of Otolaryngology, Vanderbilt University Medical Center, and †Department of Electrical Engineering and Computer Science, Vanderbilt University, Nashville, Tennessee, U.S.A.*

Hypothesis: We hypothesize that surface landmarks surrounding the round window typically used to guide electrode placement during cochlear implantation (CI) exhibit substantial variability with respect to intracochlear anatomy.
Background: Recent publications suggest that both atraumatic electrode insertion and electrode location within the scala tympani can affect auditory performance after CI. However, current techniques for electrode insertion rely on surface landmarks alone for navigation, without actual visualization of intracochlear structures other than what can be seen through a surgically created cochleostomy. In this study, we quantify how well the position of intracochlear anatomy is predicted by surface landmarks surrounding the round window.
Methods: Structures representing middle ear surface and intracochlear anatomy were reconstructed in μCT scans of 10 temporal bone specimens. These structures were then reoriented into a normalized coordinate system to facilitate measurement of intersubject anatomical shape variations.
Results: Only minor intersubject variations were detected for intracochlear anatomy (maximum deviation, 0.71 mm; standard deviation, 0.21 mm), with greatest differences existing near the hook and apex. Larger intersubject variations in intracochlear structures were detected when considered relative to surface landmarks surrounding the round window (maximum deviation, 0.83 mm; standard deviation, 0.54 mm).
Conclusion: The cochlea and its scala exhibit considerable variability in relation to middle ear surface landmarks. While support for more precise, atraumatic CI electrode insertion techniques is growing in the otologic community, landmark guided insertion techniques have limited precision. Refining the CI insertion process may require the development of image-guidance systems for use in otologic surgery. **Key Words:** Anatomic variability—Cochlear anatomy—Cochlear implant—Electrode insertion—Middle ear surface anatomy.

Otol Neurotol **34:**1675–1680, 2013.

With advances in both implant design and surgical technique, audiologic outcomes after cochlear implantation have improved significantly over time. As a result, current criteria for implantation have now been extended to include patients with less than profound levels of deafness. For the growing number of patients with residual acoustic hearing who undergo CI, it is increasingly being demonstrated that multiple audiologic benefits may be derived from preservation of this hearing. Several reports have shown combined electrical and acoustic stimulation to improve the perception of various complex auditory stimuli, such as understanding speech in the presence of background noise, music appreciation, and sound localization (1,2). Additionally, another study has suggested that minimizing trauma during electrode insertion (as indicated by preserved hearing) may improve the effectiveness of electrical stimulation alone, with a resulting benefit to audiologic outcomes (3).

Among the multiple etiologies of hearing loss during CI, acute mechanical trauma from electrode placement plays a major role. Electrode insertion has the potential to disrupt the osseous spiral lamina, spiral ligament, stria vascularis, and/or basilar membrane, all of which can lead to loss of residual hearing (4,5). Moreover, it has been demonstrated that partial electrode insertion into the scala

Address correspondence and reprint requests to Stanley Pelosi, M.D., Department of Otolaryngology–Head and Neck Surgery, Vanderbilt University Medical Center, 7209 Medical Center East-South Tower, 1215 21st Avenue South Nashville, TN 37232; E-mail: stanley.pelosi@vanderbilt.edu
Stanley Pelosi and Jack H. Noble: are co-first authors; both authors contributed equally to preparation of this article.
Outside funding: This work was supported by NIH grants R01EB006193 from the National Institute of Biomedical Imaging and Bioengineering, and R21DC012620 and R01DC008408 from the National Institute of Deafness and Other Communication Disorders.
Other disclosures/potential conflict of interests: Robert F. Labadie, MD, PhD, Advisory Board for Med-El, Ototronix; Consultant for Cochlear.

vestibuli occurs in a substantial percentage of cochlear implant surgeries (6). Many hearing preservation efforts have hence focused on modifications in electrode design and surgical insertion technique to minimize trauma.

The current method for electrode insertion relies on surface landmarks surrounding the round window alone to predict the orientation of intracochlear structures, without actual visualization of the scala tympani other than what can be seen through a surgically created cochleostomy. The consistency of these surgical landmarks in relation to the orientation of intracochlear structures is uncertain. Moreover, studies of the human cochlea have shown variability between patients in its anatomic components, including basal segment length, diameter, and turning radius (7). Together with such intracochlear variations, inconsistency in the relation of middle ear surface structures to the scala tympani might further contribute to intracochlear trauma during electrode insertion.

In this study, we quantify how well the position of intracochlear anatomy is predicted by middle ear landmarks surrounding the round window. We use rigid and nonrigid image registration techniques to estimate average cochlear anatomy from μCTs of a group of 10 temporal bone specimens and then measure the variations from the average shape across the group of specimens. Our hypothesis is that the surface landmarks typically used to guide electrode placement during cochlear implantation (CI) exhibit substantial variability with respect to intracochlear anatomy.

METHODS

Ten human cadaveric temporal bones were obtained from the Vanderbilt University School of Medicine's Anatomical Gift Program. The cochlea specimens were harvested from each cadaver using a bone saw. Each cochlea underwent computed tomography using a μCT scanner (Scanco, voxel size 36 um isotropic). The μCT scan provides sufficient detail to visualize the basilar membrane, allowing for manual delineation of structures representing the scala vestibuli, scala tympani, and middle ear surface anatomy in each specimen (Fig. 1).

Establishing a point correspondence across the set of specimens is necessary to analyze anatomical variations. A point correspondence was established using a sequence of automated and manual steps that match points on the surfaces of the structures of interest in one μCT chosen as a ''reference volume'' to surface points in each other μCT (''training volumes''). First, rigid (8) and nonrigid (9) registration of the reference volume to each training volume was performed using intensity-based methods described in previous work (10). Rigid registration aligns structures through the processes of translation and rotation. The subsequent nonrigid registration step accounts for intersubject variations in intracochlear shape that are nonlinear, allowing for more complex warping between images. Next, the structure surfaces in the reference volume were projected onto each training volume through the corresponding registration transformation, and any visually identifiable errors from the rigid/nonrigid registration process were corrected by further deforming the reference surfaces manually to match the structure surfaces that were delineated in the training volume using software designed for this purpose. Finally, a correspondence is established by associating each *i*th point on the reference surface with the point on the training volume surface that is closest to the deformed *i*th reference surface point.

Once a point correspondence for the structures of interest across specimens is established, the manually delineated structure surfaces from each specimen can be registered into a normalized coordinate space to facilitate estimating the average anatomy shape and measuring shape variations across specimens. In this work, we created 2 coordinate spaces to measure shape variations in 2 ways. First, we create a coordinate space in which variations in intracochlear anatomy can be measured with reference to middle ear surface points surrounding the round window (Fig. 2). Because these points provide surface landmarks for cochlear implant electrode insertion, this is equivalent to measuring variations in

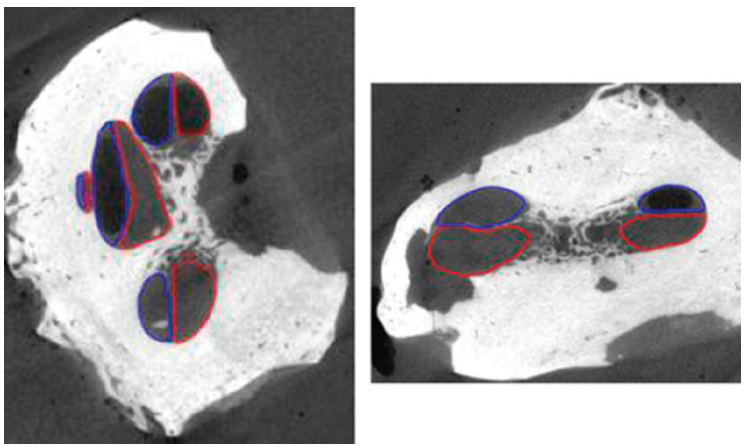

FIG. 1. Shown in the figure are a sagittal (*left*) and axial (*right*) cut of a micro-CT volume of one of the specimens used in this study. Also shown are contours around the manually delineated scala tympani (*red*) and scala vestibuli (*blue*).

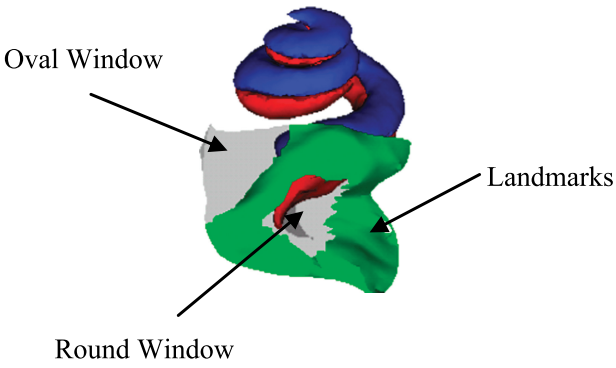

FIG. 2. This image depicts the middle ear surface landmarks (*green*) surrounding the round window overhang that were used to optimally align individual temporal bone specimen images.

cochlear anatomy with respect to surgical landmarks. To create this normalized space, we bring the structure surfaces from each of the 10 specimens into alignment with the registration transformations that optimally align the surface points surrounding the round window across specimens using point-distance-minimization techniques (11). Second, we create a coordinate system in which variations in intracochlear anatomy can be measured with reference to the cochlea. This aims to estimate the true anatomic variability in the scalae across subjects. The space is created by bringing the surfaces from each specimen into alignment with the registration transformations that optimally align points in the scala tympani and scala vestibuli surfaces across specimens using the same point registration techniques as above. Once the 2 shape spaces are created, the average shape and shape variations in each space can be estimated by computing these statistics on the registered corresponding points.

For both scalae, the maximum and standard deviation of the distance from a point in the mean shape to corresponding points in individual specimens were then calculated in both reference spaces. These measures were used to represent the amount of positional variation at a particular location in the average shape.

We also determined the optimal electrode insertion trajectory for average anatomy specified in the middle ear surface landmarks reference space and applied this trajectory to individual cases. The optimal electrode insertion trajectory was defined as the trajectory that points at a tangential angle down the middle of the basal turn of the average scala tympani shape. When applied to individual cases, the insertion trajectory passed through the identical corresponding middle ear surface points as the mean shape and was directed in the same orientation, effectively reproducing an identical surgical approach for each individual temporal bone specimen.

All software used for image processing was written in the laboratory using C++. Visualizations were created using the Visualization Toolkit library (12).

RESULTS

We found relatively little variation between individual specimens when assessing intracochlear shape with respect to the cochlea itself. Table 1 demonstrates that for corresponding points between specimens, the maximum distance from the average shape was 0.47 for the scala tympani and 0.71 for the scala vestibuli. The greatest variability in points was found in the hook region of the basal turn for both scala (Fig. 3, left). The overall standard deviation from the average shape was 0.21 mm for the cochlea as a whole.

When considering the positioning of intracochlear structures relative to surface structures surrounding the round window, we found greater intersubject variation. Table 1 shows that using these points to register the scalae resulted in a greater overall standard deviation (0.53–0.54 mm) from the average shape of the cochlea. The maximum distance from the average shape was also greater (0.81 mm for the scala vestibuli and 0.83 mm for the scala tympani). Variability tended to increase with greater anatomic distance from surface structures surrounding the round window, being most significant in the distal aspect of the basal turn (Fig. 3, right).

In applying the optimal electrode insertion trajectory of the mean shape to individual cases, we found that the ideal surgical approach for the average case does not ensure ideal electrode placement for individual cases. The bottom panel in Figure 4 provides a rendering of the average anatomy (using a right cochlea as the reference volume) and its optimal electrode insertion trajectory. Above this image are renderings of the cochlea and middle ear surface anatomy for each training volume, numbered 1 to 10. Superimposed on these figures is the optimal electrode insertion trajectory based on average anatomy. The figures demonstrate that in most cases, improvements in either entry point or entry angle could be made to improve the accuracy of electrode insertion into the scala tympani. For individual volumes 2, 4, and 9, the insertion trajectory overlaps with the scala vestibuli, creating potential for basilar membrane disruption and/or scala vestibuli entry during electrode placement. In the posterior-anterior views, a trajectory that is too far superior (Volumes 1, 5, and 8) increases the possibility of modiolar injury, whereas one that is too inferior (Volumes 2 and 3) enhances the likelihood of lateral wall trauma. A final observation to be made from the posterior-anterior renderings is that each training volume has a variable

TABLE 1. *Mean and maximum deviations (mm) in the position of the scala tympani and scala vestibuli when measured with respect to surgical landmarks, that is, middle ear surface anatomy, and when measured with respect to the cochlea*

Reference		Surgical landmarks		Cochlea	
		Mean	Max	Mean	Max
Scala tympani	Overall	0.53	0.83	0.21	0.47
Scala vestibuli		0.54	0.81	0.21	0.71
Scala tympani	Base	0.34	0.49	0.25	0.47
Scala vestibuli		0.38	0.80	0.27	0.71
Scala tympani	Apex	0.56	0.71	0.21	0.45
Scala vestibuli		0.55	0.71	0.19	0.34

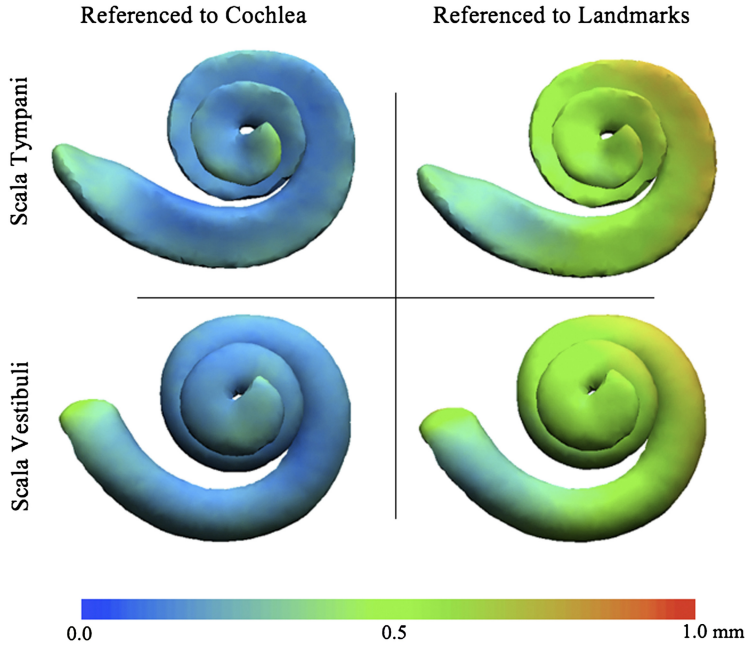

FIG. 3. Shown in the figure are 3D renderings of the average shape of the scala tympani and scala vestibuli. The color at each point on the surfaces corresponds to the mean deviation (in mm) of the position of that point on the structure when measured with respect to surgical landmarks, that is, surface structures surrounding the round window (*right column*), and when measured with respect to the cochlea (*left column*).

basal turn length and turning radius, creating further potential for electrode insertion trauma using a fixed approach.

DISCUSSION

The purpose of this study was to assess the relationship between intracochlear scala and surface structures surrounding the round window. We hypothesized that substantial variability would exist between these structures, and our results confirm this hypothesis, showing that the standard deviation from the average intracochlear shape is greater when measured in reference to middle ear surface landmarks compared with referencing to the cochlea alone. We found that points in the basal turn of the scala tympani can exhibit variability of up to approximately 0.5 mm relative to middle ear surface structures surrounding the round window. When considering that the intended target of electrode insertion, the basal turn, has only a diameter of 1 to 1.5 mm (13), this combination of a narrow target with uncertainty in accurate identification of the target creates a substantial likelihood of electrode insertion trauma. Moreover, our renderings of the optimal insertion trajectory based on an ''average'' cochlea suggest that an identical electrode insertion approach based on surface landmarks alone may result in suboptimal electrode placement for a number of patients, resulting in trauma to the basilar membrane, modiolus, and/or lateral scalar wall.

Interpatient variations between intracochlear structures and surface landmarks surrounding the round window are just one potential source of anatomic variability encountered during the electrode insertion process. The relation of the facial nerve to intracochlear scala may also affect electrode insertion trajectory. It has been shown that, for many individuals, the optimal insertion vectors resulting in centerline basal segment scala tympani insertion will intersect with the facial nerve (14). One means of addressing such anatomic constraints posed by the facial nerve may involve use of flexible electrode arrays that can bend to provide an improved insertion trajectory in the space between the facial recess and the cochlea.

Our finding that interpatient variations exist when assessing intracochlear shape with respect to the cochlea itself is consistent with anatomical variability in other studies of cochlear specimens without known ear disease (7). It should be also acknowledged that this intracochlear variability may be even greater for the subset of CI candidates with congenital hearing loss. One study showed that patients with underdeveloped cochleae (as marked by the absence of an interscalar septum) demonstrate a smaller cochlear basal segment and a reduced angle between the first and second turns (15). Such added variation further enhances the potential for trauma during electrode insertion.

The results presented have important implications for electrode insertion techniques related to cochlear implantation. Because of the poor reliability of standard insertion methods in minimizing intracochlear trauma, going forward alternate strategies will require consideration to improve hearing preservation outcomes after CI. Image-guided technologies remain in a state of infancy but hold promise as one means of improving the location and trajectory of electrode insertion techniques so as to minimize trauma. Recent preliminary efforts from the authors have used a

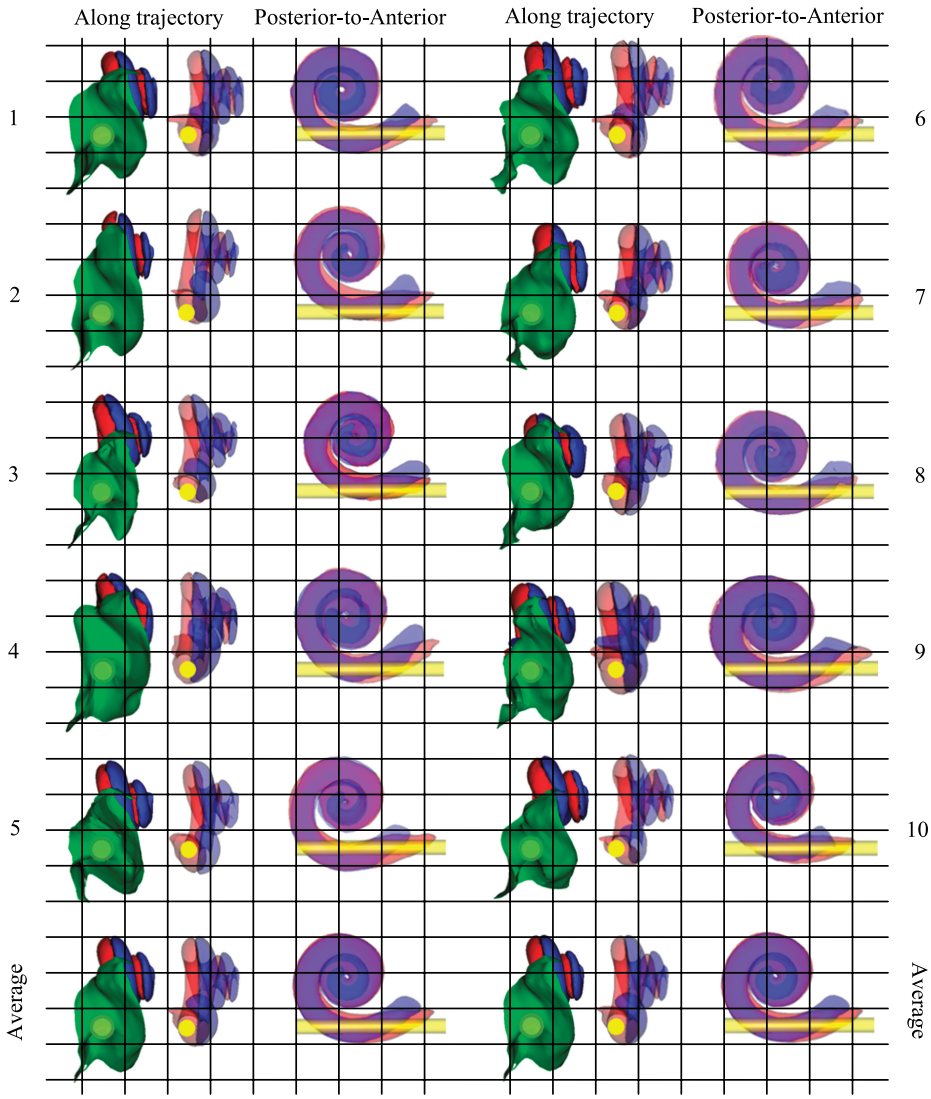

FIG. 4. Shown in the figure are 3D renderings of middle ear surface structures surrounding the round window (*green*), scala tympani (*red*) and scala vestibuli (*blue*) from all 10 volumes registered with respect to the middle ear surface structures. The bottom row shows the average shape from Volumes 1 to 10. Also shown is a 1-mm diameter yellow tube that represents the optimal electrode insertion trajectory in average anatomy.

virtual image guidance model to show that knowledge of subsurface anatomy during electrode insertion facilitates complete scala tympani insertion while minimizing basilar membrane disruption (16). Additionally, this enhanced knowledge of underlying scalar anatomy was found to improve consistency between surgeons in electrode insertion trajectory. Such improved consistency in surgical technique, together with refinement in electrode design, will ultimately be necessary at a clinical level to improve the reliability of hearing preservation outcomes.

We acknowledge some inherent study design limitations. Although use of rigid and nonrigid image registration techniques is a validated method of establishing point correspondence between radiographic specimens, this process may require manual adjustments that can introduce variability into results. Also, our rendering of electrode insertion trajectory based on average cochlear shape is intended to simulate a standardized approach for electrode insertion; however, such a scenario rarely exists in reality as techniques of insertion typically vary between different surgeons and, for individual surgeons, between individual cases.

CONCLUSION

The cochlea and its scalae exhibit considerable variability in relation to middle ear surface landmarks surrounding the round window. Although support for more

precise, atraumatic CI electrode insertion techniques is growing in the otologic community, landmark-guided insertion techniques have limited precision. Refining the CI insertion process may require the development of image-guidance systems for use in otologic surgery.

REFERENCES

1. Gantz BJ, Turner C, Gfeller KE, Lowder MW. Preservation of hearing in cochlear implant surgery: advantages of combined electrical and acoustical speech processing. *Laryngoscope* 2005;115:796–802.
2. Dunn CC, Perreau A, Gantz B, Tyler RS. Benefits of localization and speech perception with multiple noise sources in listeners with a short-electrode cochlear implant. *J Am Acad Audiol* 2010;21:44–51.
3. Carlson ML, Driscoll CL, Gifford RH, et al. Implications of minimizing trauma during conventional cochlear implantation. *Otol Neurotol* 2011;32:962–8.
4. Roland PS, Wright CG. Surgical aspects of cochlear implantation: mechanisms of insertional trauma. *Adv Otorhinolaryngol* 2006;64: 11–30.
5. Briggs RJ, Tykocinski M, Xu J, et al. Comparison of round window and cochleostomy approaches with a prototype hearing preservation electrode. *Audiol Neurotol* 2006;11:42–8.
6. Aschendorff A, Kromeier J, Klenzner T, Laszig R. Quality control after insertion of the nucleus contour and contour advance electrode in adults. *Ear Hear* 2007;28:75S–9.
7. Erixon E, Hogstorp H, Wadin K, Rask-Andersen H. Variational anatomy of the human cochlea: implications for cochlear implantation. *Otol Neurotol* 2009;30:14–22.
8. Maes F, Collignon A, Vandermeulen D, Marchal G, Suetens P. Multimodality image registration by maximization of mutual information. *IEEE Trans Med Imaging* 1997;16:187–98.
9. Rohde GK, Aldroubi A, Dawant BM. The adaptive bases algorithm for intensity-based nonrigid image registration. *IEEE Trans Med Imaging* 2003;22:1470–9.
10. Noble JH, Labadie RF, Majdani O, Dawant BM. Automatic segmentation of intra-cochlear anatomy in conventional CT. *IEEE Trans Biomed Eng* 2011;58:2625–32.
11. Arun KS, Huang TS, Blostein SD. Least square fitting of two 3-D point sets. *IEEE Trans Pattern Anal Mach Intell* 1987;9:698–700.
12. Schroeder W, Martin K, Lorensen B. *The Visualization Toolkit*, 3rd ed. Clifton Park, NY: Kitware, 2003.
13. Biedron S, Prescher A, Ilgner J, Westhofen M. The internal dimensions of the cochlear scalae with special reference to cochlear electrode insertion trauma. *Otol Neurotol* 2010;31:731–7.
14. Meshik X, Holden TA, Chole RA, Hullar TE. Optimal cochlear implant insertion vectors. *Otol Neurotol* 2010;31:58–63.
15. Martinez-Monedero R, Niparko JK, Aygun N. Cochlear coiling pattern and orientation differences in cochlear implant candidates. *Otol Neurotol* 2011;32:1086–93.
16. Noble JH, Labadie RF, Wanna GB, Dawant BM. Image guidance could aid performance of atraumatic cochlear implantation surgical techniques. Presented at SPIE Conf on Medical Imaging. 2013.